Temperature or Transport? Range Limits in Marine Species Mediated Solely by Flow

Brian Gaylord[1] and Steven D. Gaines

Department of Ecology, Evolution, and Marine Biology, University of California, Santa Barbara, California 93106

Submitted April 26, 1999; Accepted December 23, 1999

ABSTRACT: Clusters of range boundaries in coastal marine species often occur at shoreline locations where major nearshore ocean currents collide. Observing that these currents are typically composed of waters with quite different physical characteristics, biologists have traditionally assumed that high local densities of marine range limits result primarily from the strong water property gradients (particularly in temperature) that arise at oceanographic discontinuities. However, this view may overlook the potential for ocean flows themselves to generate distributional pattern. Here we explore this possibility in more detail using an extension of a coupled population dispersal model developed previously for benthic marine species with dispersing larvae. Results suggest that simple, common flow fields often observed in association with biogeographic boundaries worldwide may have the potential to constrain a species' geographic range, even when suitable habitat outside that range is abundant. Model predictions suggest that these boundaries can function as one- or two-way barriers to range expansion and may be differentially permeable, with boundary leakiness depending on life-history characteristics and the degree of temporal variability in the nearshore flow field.

Keywords: physical-biological coupling, dispersal, biogeography, recruitment, oceanography.

It is well recognized that species' range limits are not uniformly distributed in space. For example, species' boundaries tend to become more densely packed as one approaches the equator (Pianka 1988). Range borders also often cluster at particular locations, defining sharp discontinuities between biogeographic provinces (Pielou 1979). Both terrestrial and marine taxa show these trends. However, subtle differences may exist as well in the distributional character of species on land and in the sea. Marine taxa, for instance, include several of the more prominent exceptions to the rule that species diversity increases in the Tropics (e.g., Gaines and Lubchenco 1982). Similarly, a number of the clearest counterexamples to observed patterns of equatorward reduction in north-south range breadth (Rapoport 1982; Stevens 1989) appear in coastal ocean species (Rohde et al. 1993; Roy et al. 1994; Stevens 1996).

Such terrestrial-marine distributional differences are perhaps not surprising since distinct mechanisms may work to generate range structure in these two realms. Consider, for example, factors leading to clustering of distributional boundaries. On land, critical habitat characteristics can change drastically over short distances because of explicit barriers such as mountains, deserts, and watergaps. In other cases, the bunching of terrestrial range limits may derive from historical events such as glacial intrusion or land bridge submergence (Pielou 1979). In marine systems, however, it becomes more difficult to envision how persistent range boundaries can become locally concentrated. Although substrate types vary spatially and rivers alter local salinity levels, a single, continuous, dispersal medium (the ocean) connects all available habitat, and environmental gradients within this medium are neither as striking nor as immutable as on land.

Nevertheless, distributional limits in many seaweeds, intertidal and subtidal invertebrates, and coastal fishes do cluster at particular shoreline locations (Valentine 1966; Van den Hoek 1975; Hayden and Dolan 1976; Horn and Allen 1978; Murray and Littler 1981; Roy et al. 1998). Such boundaries are often associated with persistent nearshore oceanographic discontinuities. For example, a major faunal break occurs at Cape Hatteras on the east coast of the United States (e.g., Roy et al. 1998) where the Gulf Stream diverges from the coast as it collides with the lower leg of the Laborador Current (Loder et al. 1998). A similar flow regime exists off the coast of South America where the Peru Current meets the North Equatorial Countercurrent (Strub et al. 1998); this location is also considered an important biogeographic boundary (Briggs 1974). Fig-

[1] To whom correspondence should be addressed; e-mail: gaylord@lifesci.ucsb.edu.

Am. Nat. 2000. Vol. 155, pp. 769–789.

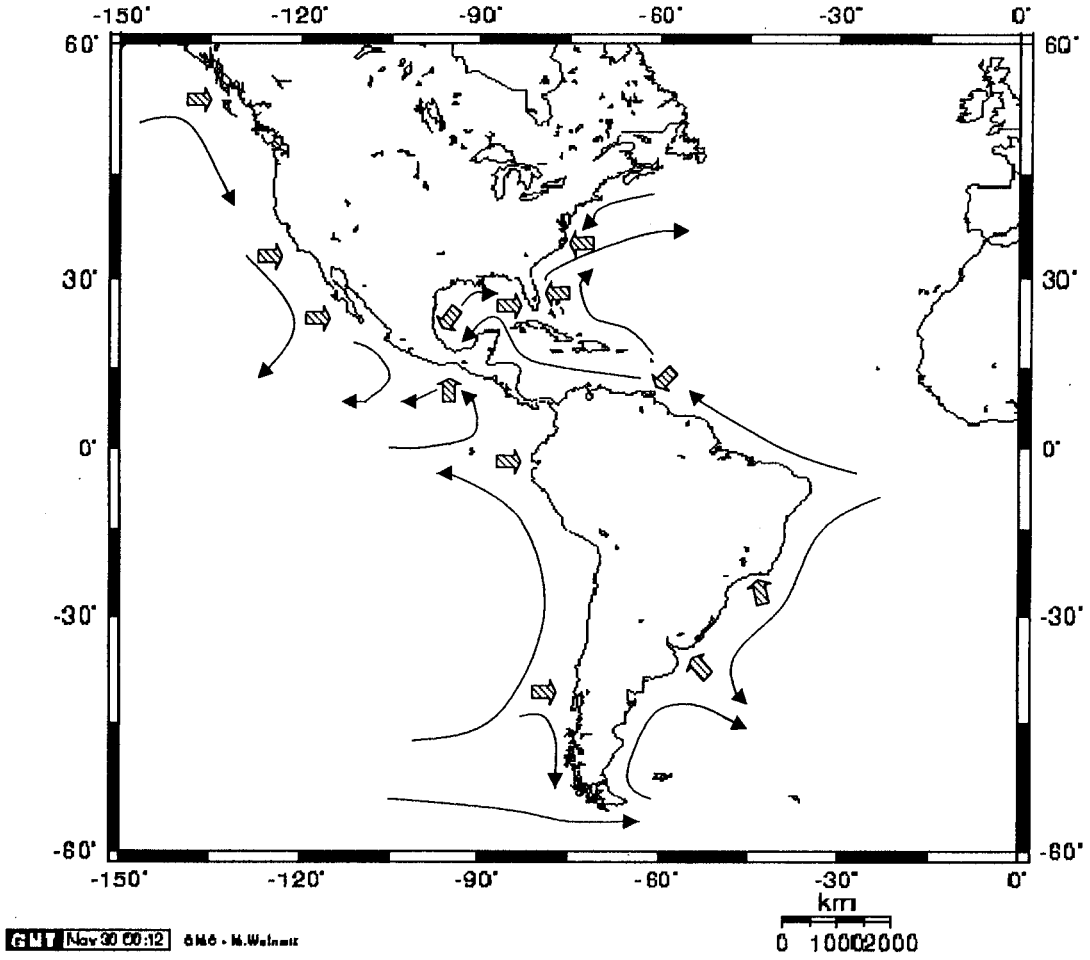

Figure 1: Marine biogeographic boundaries in the Western Hemisphere (after Briggs 1974). Note the tendency for these boundaries to occur where major currents interact.

ure 1 presents additional boundaries in the Western Hemisphere, together with major ocean current trajectories (Pickard and Emery 1990) that occur in their vicinities.

In analogy with terrestrial systems where patterns of range often track variation in habitat quality (e.g., Brown 1984), the association between nearshore current features and clusters of range borders is typically assumed to be a consequence of the gradients in water properties that arise at major current interfaces. Because large-scale ocean flows originate at different latitudes and depths, they are composed of water masses with distinct characteristics (McGowan 1971; Pond and Pickard 1983; Longhurst 1995). In particular, their temperatures are usually quite different. As a result, nearshore collisions of currents generate steep water temperature changes over short stretches of coastline. Biologists have traditionally assumed that these abrupt temperature shifts impose physiological challenges on some subset of the marine organisms living in these regions (e.g., Hutchins 1947; Hedgepeth 1957; Hayden and Dolan 1976; Suchanek et al. 1997; but see Clarke 1993), producing a high density of range limits and creating a biogeographic boundary (Pielou 1979).

Note, however, that this view ignores the potential for flow fields themselves to affect population distributions. Because a dominant fraction of marine species have dispersing larvae (Thorson 1950; Scheltema 1971; Jablonski and Lutz 1983), there is clearly a capacity for ocean flows to affect abundance patterns through their influence on recruitment processes. This raises the question as to whether certain current patterns may have the potential to generate range limits in taxa with pelagic young even when species' demographic parameters are insensitive to water property gradients.

Although the role of ocean currents in creating spatial

patterns of larval settlement has received some attention in the recent literature (e.g., Pielou 1979; Gaines and Bertness 1992; Caley et al. 1996; Menge et al. 1997), quantitative studies evaluating explicitly the consequences of directional transport are relatively rare (e.g., Hill 1991*a*; Richards et al. 1995). Indeed, many studies exploring costs and benefits of dispersal neglect advective processes entirely, assuming instead a purely diffusive dispersal pattern with no mean displacement (e.g., Palmer and Strathmann 1981; Etter and Caswell 1994). However, as suggested in an earlier mathematical model by Possingham and Roughgarden (1990), advective ocean currents may have a strong potential to influence adult shoreline abundance and distribution in species that have planktonic larvae.

Here we explore the possible theoretical role of ocean circulation on geographical distribution in more detail using a modified version of Possingham and Roughgarden's (1990) original advection-diffusion approach. In particular, we focus on the ability of a flow field, apart from any gradient in temperature or other environmental factor associated with habitat quality, to generate range boundaries in marine species that have a planktonic life-history phase. As a first step, we limit ourselves to simulations using simple representations of current fields often found in association with biogeographic boundaries worldwide, since they appear to have the greatest potential for generating constraints on range. We find that circulation patterns per se can play a surprisingly strong role in setting species geographical distribution.

The Model

The model we employ is an extension of a construct first presented by Roughgarden et al. (1988) and developed more fully by Possingham and Roughgarden (1990). This approach explores the population dynamics of a marine species with a dispersing larval phase by explicitly linking temporal changes in an adult shoreline distribution to offshore concentrations of larvae produced by those adults. The temporal and spatial pattern of larval concentration is described by a two-dimensional advection-diffusion equation (which assumes implicitly that larvae remain within a single horizontal layer of the water column or are well mixed vertically in water of nearly constant depth):

$$\frac{\partial L}{\partial t} = K\left[\frac{\partial^2 L}{\partial x^2} + \frac{\partial^2 L}{\partial y^2}\right] - u\frac{\partial L}{\partial x} - v\frac{\partial L}{\partial y} - \lambda L, \qquad (1)$$

where L is the larval concentration per unit area of ocean; K is the eddy diffusivity, an index describing the intensity of turbulent mixing; u is eastward velocity; v is northward velocity; and λ is the larval death rate. The first term (in brackets) on the right-hand side of equation (1) represents turbulent diffusion, while the second and third terms describe changes in concentration caused by advective transport of larval gradients. The fourth term accounts for loss of larvae because of mortality. All variables in equation (1) are functions of x, y, and t, except for K and λ, which are held constant. x and y coordinates are defined in figure 2.

To isolate the influence of larval dispersal on species distribution, we assume a life cycle with a sessile adult phase:

$$\frac{\partial B}{\partial t} = cFL_{\text{shore}} - \mu B, \qquad (2)$$

where B is the density of adults per unit length of coastline, c is a settlement coefficient that quantifies the propensity of larvae to settle onto the shore, F is the amount of free

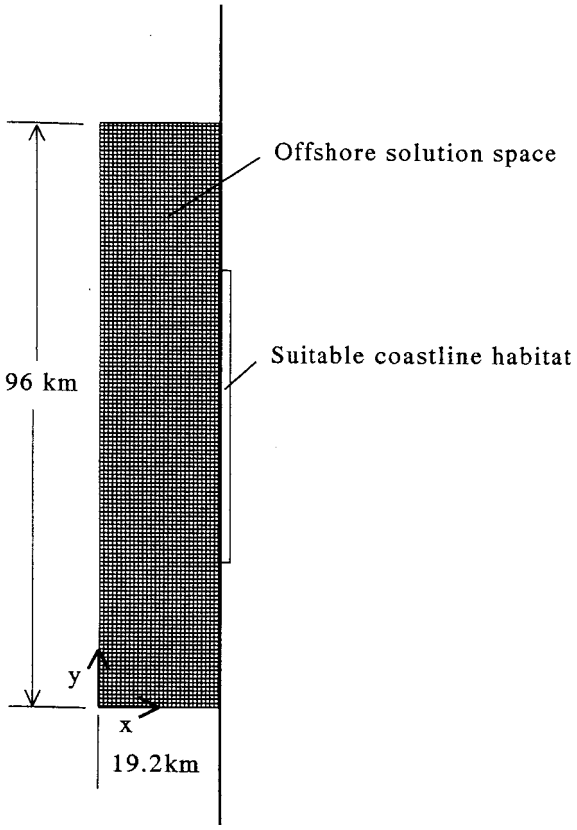

Figure 2: Geometry of the model solution space. Suitable adult habitat is assumed to exist only along the central region of the coastline. The grid spacing shown in the offshore region (where currents and turbulent diffusion transport larvae) is approximately equivalent to that used in the numerical simulations.

space per unit length of coastline, and μ is the adult per capita mortality rate. The variable L_{shore} indicates the concentration of larvae in the water immediately adjacent to the shoreline. The first term on the right-hand side represents increases in adult density caused by larval settlement, while the second accounts for adult deaths. All quantities in this equation vary with y and t except μ and c, which are constants. The appearance of F in the first right-hand term indicates that settlement is density dependent, varying in proportion to the amount of free space available. Thus, $F = A - aB$ (see Roughgarden and Iwasa 1986), where A is the total suitable substrate area per unit length of coastline and a is the age-averaged area occupied by an adult.

The above equations are coupled through a coastal boundary condition that specifies the rate at which larvae enter and leave the water at the shoreline:

$$K\left(\frac{\partial L}{\partial x}\right)_{\text{shore}} = mB - cFL_{\text{shore}}, \tag{3}$$

where m is the per capita rate of larval production. This expression states that the net flux of larvae from the shoreline equals the difference between the production of larvae by adults and the rate at which larvae settle out of the water column into the benthic population. The additional boundary conditions required for the solution of equations (1)–(3) are defined such that $L = 0$ along the oceanic edges of the solution space (i.e., the noncoastal boundaries are absorbing). Thus, any larvae carried past the northern, offshore, and southern borders do not return to the coastal region examined in this model. We discuss the computational implications of these absorbing boundaries in "Model Solution" below.

Previous Model Implementations

In the first complete development of the above model, Possingham and Roughgarden (1990) showed how alongshore flow can influence equilibrium adult distributions at the shore by sweeping larvae downstream, setting up a gradient in settlement along a coast. Their results suggested that rapid alongshore currents might have the potential to drive populations extinct by carrying larvae away from benthic habitat and reducing recruitment to levels below that required to offset adult mortality.

More recently, using a modification of the model of Roughgarden et al. (1988) and Possingham and Roughgarden (1990; henceforth both papers together will be abbreviated PRG), Alexander and Roughgarden (1996) explore consequences of reflecting fronts offshore, suggesting that pulses of recruitment can occur when such fronts move shoreward and collide with the coast. The implication is that oceanographic upwelling and relaxation phenomena may be critical factors affecting larval recruitment. Connolly and Roughgarden (1998) also use a one-dimensional analogue of Alexander and Roughgarden's (1996) approach to examine the possibility that alongshore variation in offshore advection rate combines with competitive interactions to alter relative abundances of dominant and subordinate species along a large-scale latitudinal transect.

Together, the above papers have contributed much to our understanding of how ocean transport can influence population dynamics of a species that has a dispersing larval stage. Unfortunately, these model formulations also share some important limitations. The potential disadvantages derive from an absence in the models of developmental time lags during both the larval and adult phases. This point is perhaps most easily seen via a schematic diagram such as figure 3.

In nature, most marine invertebrate and fish larvae have an obligate developmental (i.e., precompetency) period during which they are incapable of settling (Strathmann 1987). However, the models above (fig. 3*A*) allow newly hatched larvae to settle the moment they are released into

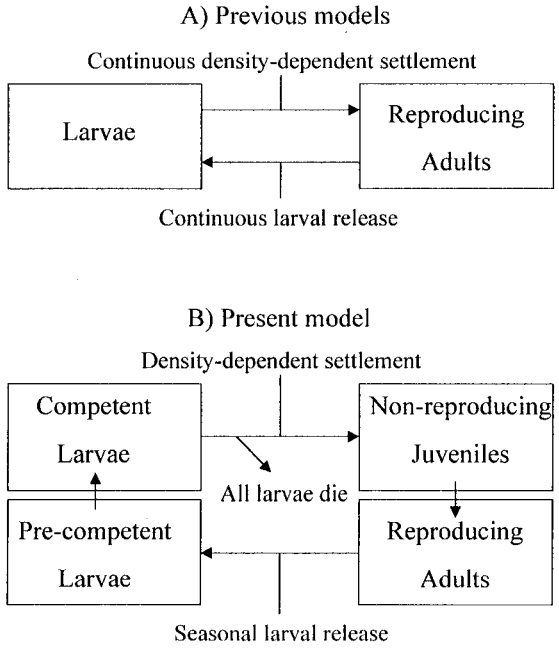

Figure 3: Schematic diagram showing model differences between implementations based on Possingham and Roughgarden (1990) and the modified formulation of this study. *A*, Original implementations with continuous larval release, the potential for immediate settlement, and instantaneous reproduction upon settlement. *B*, Present model incorporating developmental lags and finite larval life span.

the water column, become adults immediately, and give birth to their own offspring instantaneously. Not only is this feature nonbiological, it may also alter substantially the dynamics of the system. Because of the nature of diffusive processes where the net distance traveled increases roughly with the square root of time (Denny 1993), larvae tend to remain clustered near the shore for some duration after release, during which the probability of encountering the shoreline is high. Later, when larvae have diffused (and, in particular, been advected) farther from adult habitat, encounter rates decline precipitously. As a consequence, the PRG model and its descendents artificially allow large numbers of larvae to settle rapidly just after birth, while nearshore concentrations remain elevated, and before larvae have moved very far from their parents. Thus, although designed to explore the dynamics of broadly dispersing species, the structure of the PRG-type models actually precludes effective dispersal in a majority of individuals. In contrast, larvae in the real ocean may be transported (in addition to being diluted and subjected to substantial mortality) for days, weeks, or months before they become competent to settle. At such later times, coastline concentrations are much lower, settlement rates are concomitantly profoundly reduced, and individuals have often been carried much farther from their site of origin.

An analogous issue arises in the case of the adult phase. In the real world, newly settled individuals must typically pass through an explicit juvenile stage before they can reproduce. As figure 3*A* indicates, however, in the above models just-settled larvae begin producing young the instant they contact the shore. Thus, once again an important time lag present in natural populations (in this case one of several months) is eliminated.

One other disadvantage of the PRG-type models is also apparent. As noted by Jackson and Strathmann (1981), competent larvae commonly die after a finite time in the plankton if they do not settle into adult habitat. This demographic component does not appear in the above implementations, where model larvae remain competent to settle forever. Although individuals perish at some rate, making the probability of survivorship to exceptionally large ages quite low, it nonetheless remains possible for a model larva to settle even several years after birth. This feature may artificially increase settlement rates and underestimate larval wastage, as well as allowing occasional dispersal to biologically impossible distances.

In sum, although previous model versions function as valuable starting abstractions, some of their simplifications have undesirable consequences. Possingham and Roughgarden (1990) also apparently recognized some of these structural limitations, as evidenced by their use of adjusted model variables to compensate (see "Parameter Values" below). Unfortunately, the secondary modifications they employ cannot counteract fully the consequences of omitting developmental time lags.

Extended Model of This Study

Temporally Varying Components

To explore better the implications of larval dispersal, we modify the original PRG formulation to include four additional features (fig. 3*B*). First, larvae in our model are released in yearly pulses at the beginning of the reproductive season, rather than continuously (see also Richards et al. 1995). This more accurately mimics patterns observed in nature for many species, where offspring are produced seasonally. Second, released larvae initially enter a precompetency period. During this interval individuals are transported by currents and dispersed by turbulent diffusion but cannot settle even if they encounter suitable habitat. Third, larvae transition to a competency stage, during which those individuals that contact appropriate shoreline settle, exit the offshore pool, and join the benthic population. This competency period is finite; thus, all individuals that remain in the water column at the end of the competency window perish. And fourth, settled larvae pass through a several-month juvenile stage (during which they die at rate μ), before maturing to reproduce for the first time the following season. In our model, these four modifications are achieved by making the m (the adult fecundity) and c (the settlement coefficient) functions of time, with m pulsed at the beginning of each reproductive season before dropping to 0, and c nonzero only during the competency period.

Parameter Values

Table 1 shows parameter values used in our extended model as well as those employed in previous studies. Because a number of these factors differ in our model from previous implementations, and because parameters also varied among earlier versions, some discussion is warranted. In general, model variables are based on life-history characteristics of intertidal barnacles since these organisms represent one of the few cases where sufficient data exist to allow parameter estimation. We briefly address each parameter in turn.

Total available area per meter of shoreline is A. For simplicity and to facilitate consistency among models, we retain the order of magnitude value employed by PRG and Alexander and Roughgarden (1996; i.e., $A = 1\ m^2\ m^{-1}$). Connolly and Roughgarden (1998) double this value.

The basal area of an adult is a. Again, because model parameters are based loosely on values appropriate for barnacle dynamics, we use an estimate of $a = 0.0001\ m^2$.

Table 1: Model parameters

		PRG	AR	CR	This study
A	Total available area per meter of shoreline, m	1	1	2	1
a	Adult basal area, m^2	1×10^{-4}	1×10^{-4}	1×10^{-4}	1×10^{-4}
λ	Larval death rate, s^{-1}	5.6×10^{-7}	5.6×10^{-7}	5.6×10^{-7}	5.6×10^{-7}
μ	Adult death rate, s^{-1}	2.8×10^{-7}	2.8×10^{-7}	8.3×10^{-8}	2.2×10^{-8}
m	Larval production rate, s^{-1}	6.7×10^{-6}	6.7×10^{-6}	4.2×10^{-6}	3.2×10^{-3}
K	Eddy diffusivity, $m^2\ s^{-1}$	10	10	10	10
c	Larval settlement rate, s^{-1}	5.6×10^{-8}	5.6×10^{-6}	Ambiguous	5×10^{-5}
d_1	Larval precompetency duration, s	…	…	…	1.8×10^6
d_2	Larval competency duration, s	…	…	…	1.8×10^6

Note: PRG: Roughgarden et al. (1988), Possingham and Roughgarden (1990). AR: Alexander and Roughgarden (1996). CR: Connolly and Roughgarden (1998).

The adult mortality rate is μ. In his classic 1961 study, Connell reports yearly survivorship rates ranging from 1% to 83%. We therefore use a baseline value of 50% (i.e., $\mu = 2.2 \times 10^{-8}\ s^{-1}$), exploring consequences of higher and lower rates as a secondary issue. Note that in order to offset the artificially high settlement and instantaneous reproduction that occurs in their models, PRG and Alexander and Roughgarden (1996) use an exceptionally high adult mortality rate corresponding to yearly survivorship of less than two one-hundredths of 1%. Connolly and Roughgarden (1998) use a value for μ that leads to yearly survivorship of 7%.

The larval production rate is m. Hines (1978) reports that a *Balanus glandula* individual of 10 mg body weight produces approximately 1×10^5 eggs yr^{-1}. Although in our model we assume adults release all larvae at the beginning of the reproductive season, in a continuous-release representation (calculated for comparison to previous models), this becomes equivalent to $m = 3.2 \times 10^{-3}\ s^{-1}$. Again, to offset overestimates of larval release caused by instantaneous reproduction by newly settled larvae, PRG, Alexander and Roughgarden (1996), and Connolly and Roughgarden (1998) reduce this value to levels almost 500–750 times smaller.

Larval settlement coefficient is c. Gaines et al. (1985) provide data yielding estimates of settlement coefficients ranging between roughly $3 \times 10^{-4}\ s^{-1}$ and $5 \times 10^{-5}\ s^{-1}$ (app. A). In our study, we use the lower of these two values. Alexander and Roughgarden (1996) employ a value almost 10 times smaller, and PRG a value nearly 1,000 times smaller. Connolly and Roughgarden (1998) appear to use the same value as PRG, but because their value is presented in incorrect dimensions, this is not entirely clear. The rationale in the previous studies for decreasing c to these smaller values seems to be based on the argument that only a tiny percentage of suspended larvae are competent to settle. However, this post hoc adjustment seems inappropriate since the field data of Gaines et al. (1985), from which the unadjusted c is computed, already incorporate any such effects. Again, these smaller settlement coefficients may have been necessary to help offset the artificially high rates of larval encounter with the shore that result from the lack of an explicit precompetency period.

The larval precompetency and competency periods are d_1 and d_2, respectively. Strathmann (1987) provides data that suggest barnacle larvae remain in the water column for approximately 3–4 wk before settling, and Jackson and Strathmann (1981) indicate that for many species, precompetency and competency durations are of similar duration. Thus, we use a baseline value of $d_1 = d_2 = 3$ wk (1.8×10^6 s) and touch secondarily on consequences of variation in this parameter.

The larval mortality rate is λ. Although field measurements of larval death rates are sparse, Pyefinch (1948) provides data with which to crudely estimate them. His data suggest a larval mortality rate of the order of 5% per day, corresponding to $\lambda = 5.6 \times 10^{-7}\ s^{-1}$. This value is the same as that used in previous models.

Horizontal eddy diffusivity is K. A reasonable nearshore value for the spatial scales we consider is $10\ m^2\ s^{-1}$ (Okubo 1971; Mann and Lazier 1996). Note, however, that the assumption of a constant K is a substantial simplification (see, e.g., Wroblewski and O'Brien 1981; Richards et al. 1995; and "Discussion" below) and serves again to emphasize the essentially illustrative character of the model developed here.

Flow Fields

Four simple representations of current patterns associated with biogeographic boundaries are tested in our study (fig. 4). Although these crude representations of $u(x, y)$ and $v(x, y)$ clearly do not contain the fine or mesoscale complexity found in nature, they provide phenomenological flow "cartoons" that incorporate the dominant features of several common large-scale flow fields. The first velocity

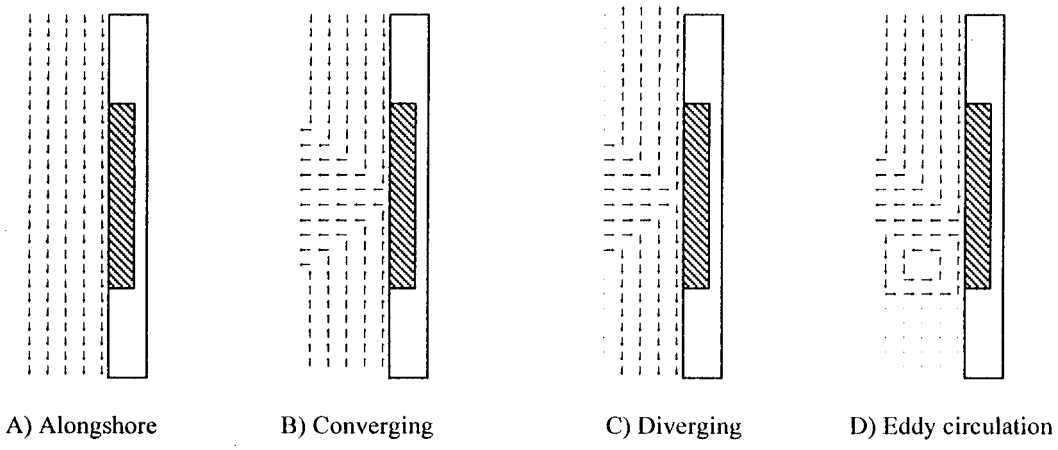

Figure 4: Simplified phenomenological flow "cartoons" representing common coastal oceanographic features often associated with marine biogeographic boundaries. Higher-resolution equivalents to these flow fields define u and v in equation (1).

field (alongshore flow) is essentially a default case, a unidirectional current parallel to the shoreline. The second flow pattern (converging flow) approximates the head-on collision of two alongshore currents, perhaps reminiscent of the pattern of flow mentioned earlier, where the Gulf Stream and the Laborador Current meet on the east coast of the United States. The third flow situation (diverging flow) represents the direct impingement of a current against a coast, followed by its splitting into two oppositely directed alongshore components. This situation may mimic crudely the fluid movement along the coast of Chile where the West Wind Drift runs against South America and diverges into northward and southward arms (Strub et al. 1998). Finally, the fourth flow case (eddy circulation) approximates alongshore flow departing from a coast (perhaps caused by an unspecified topographical feature not explicitly represented on our simplified coastline), producing a recirculating eddy in its lee. We discuss this flow field in more depth below.

Model Solution

Equations (1)–(3), incorporating the flow fields described above, are solved on a two-dimensional grid using standard finite difference techniques (see app. B for details). An alternating direction implicit method (Ferziger 1981) is employed to solve equation (1), and a standard implicit approach is applied to equation (2). The link between the two expressions is handled using an iterative convergence scheme since equation (2) and the coastal boundary condition (eq. [3]) contain elements that act like nonlinearities because of the product of B and L in the cFL_{shore} terms. To minimize artificial loss of larvae from the absorbing boundaries of the finite computational domain, we assume (as in PRG) that only the central 50% of the coastline contains suitable habitat ($A = 0$ elsewhere). This localizes the region of important dynamics far enough from the oceanic boundaries that edge effects do not materially influence model solutions, a point we have verified directly by conducting a subset of runs with larger computational domains.

Results

Basic Flow Regimes

Alongshore Flow. Figure 5 shows the adult shoreline distributions that arise from uniform alongshore flow. At a flow speed of 0.25 cm s^{-1}, adult abundance increases rapidly from an initial 10% cover to an equilibrium level of approximately 50%. For 1 cm s^{-1} flows, however, the adult distribution slides downstream and eventually declines to extinction (defined for convenience here as adult cover below 0.02%). At an even faster flow rate of 4 cm s^{-1}, larvae are swept so rapidly downstream that virtually none are able to settle within the region of suitable habitat and the population goes extinct as if reproduction were 0.

Converging Flow. Figure 6 shows analogous results for the case of colliding alongshore currents. Under these conditions, slow flows (0.25 cm s^{-1}) again allow the adult population to increase rapidly to equilibrium levels and persist through time. At intermediate flows rates (1 cm s^{-1}), the adult distribution compresses into the center of suitable habitat but then decreases in abundance and goes extinct. The extinction progression again occurs more rapidly for 4 cm s^{-1} flows.

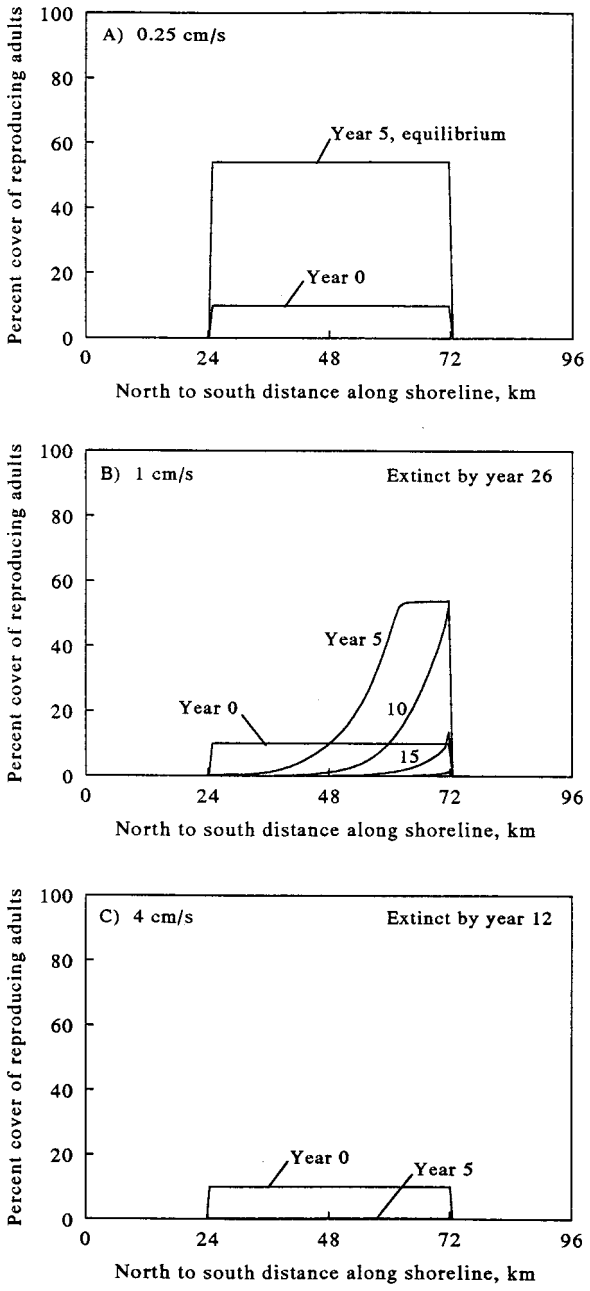

Figure 5: Adult shoreline distributions resulting from uniform alongshore flow.

Diverging Flow. A similar pattern arises in the diverging flow case, as well (fig. 7). Slower flows again enable the adult population to increase rapidly from an initial low abundance to an equilibrium level, and faster velocities again cause extinction. In this case, the highest abundances during an extinction trajectory occur at the upstream and downstream limits of suitable habitat.

These first three flow cases indicate (as originally suggested by the model of PRG) that alongshore currents may be of critical importance for determining the persistence of marine species with dispersing larvae. This study suggests, in fact, that populations may be more sensitive to the presence of rapid alongshore fluid movement than initially supposed. This exacerbated vulnerability to ad-

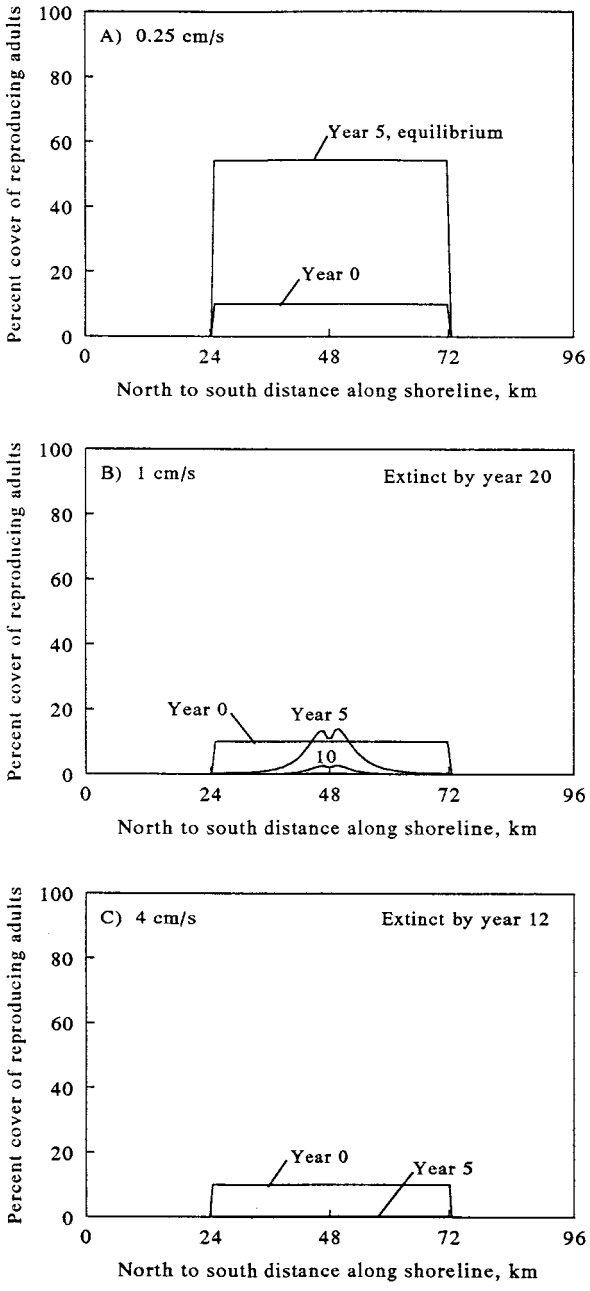

Figure 6: Adult shoreline distributions resulting from a converging flow field.

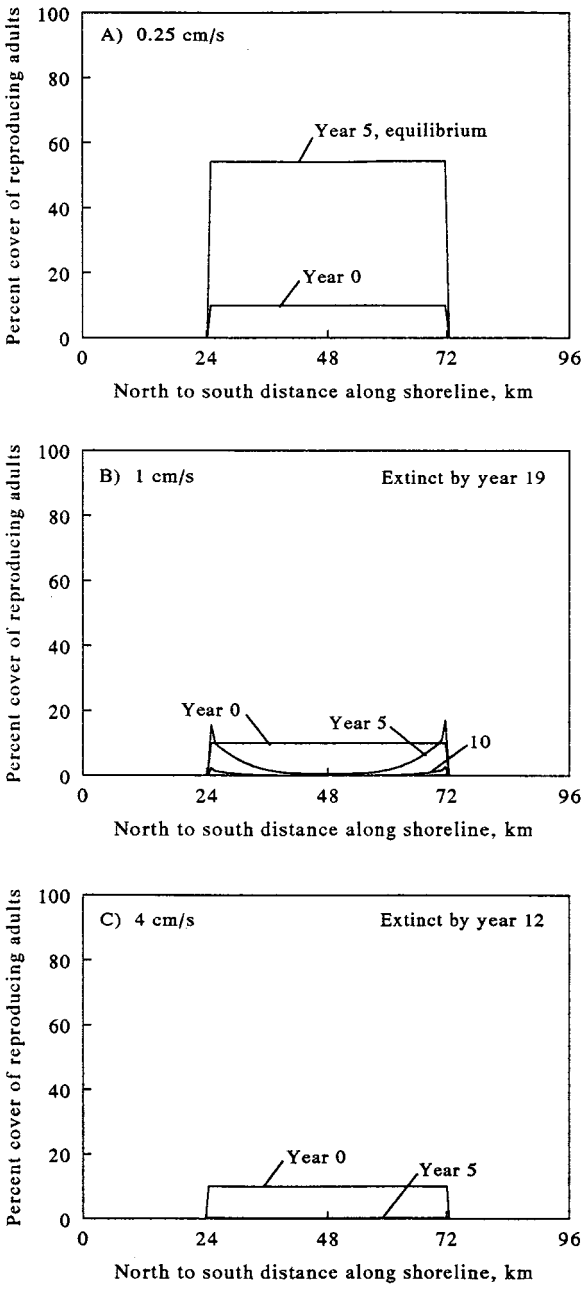

Figure 7: Adult shoreline distributions resulting from a diverging flow field.

vection arises predominantly from the time lag between larval release and settlement, which causes larvae to be diluted, swept farther from suitable habitat, and subjected to high larval mortality before they can settle.

It is perhaps important to emphasize that the above critical current speeds for population persistence are not at all rapid for flows in the ocean. The rate of 4 cm s^{-1} is a typical velocity magnitude present in many coastal environments, and speeds an order of magnitude faster can be found along many of the world's shores. The above results, therefore, raise the question of how populations persist in the face of actual currents in nature. One possibility (we discuss others in the "Discussion") is that many marine populations are not self-supporting but instead subsist on external larval input from upstream sources. In such a scenario, larvae advected to the vicinity of a particular habitat from upstream simply replace those that are swept downstream away from that same habitat. The greatest difficulty with this hypothesis is that it immediately raises the question of how the population furthest upstream would support itself. We now turn to an examination of a flow field that may enable a population to accomplish this feat.

Range Boundaries and Larval Sources

Figure 8 presents results from the eddy-circulation current pattern. At slow flow rates, once again the population increases rapidly to equilibrium levels and persists through time. Results for intermediate current velocities (1 cm s^{-1}) also resemble previous findings; adult abundances decline to extinction. However, a very different pattern arises at 4 cm s^{-1}, where the adult distribution declines to extinction within the northern section of habitat but increases along the southern region of shoreline adjacent to the eddy. Eventually, adult abundances in this southern portion reach similar equilibrium levels as those arising from 0.25 cm s^{-1} flows.

This is an important finding in at least two respects. First, the abundance curve of figure 8*C* provides a striking example of a sharp, distinct, flow-induced range limit (indicated symbolically by a bold arrow). This result yields the first quantitative evidence that flow alone can create range boundaries within the middle of suitable habitat, even when water mass characteristics or biological factors are ignored. Second, as alluded to above, it is possible for a population maintained by such an eddy to also function as a persistent larval source for downstream locations. Because an eddy population is self-sustaining and requires no external larval input for its persistence, all larvae that diffuse out of the recirculation zone are available for other populations. Note that the apparently anomalous intermediate flow result (i.e., eventual extinction) results from the fact that the eddy circulation rate at intermediate velocities is too slow to return larvae to the shore before the end of the larval competency period.

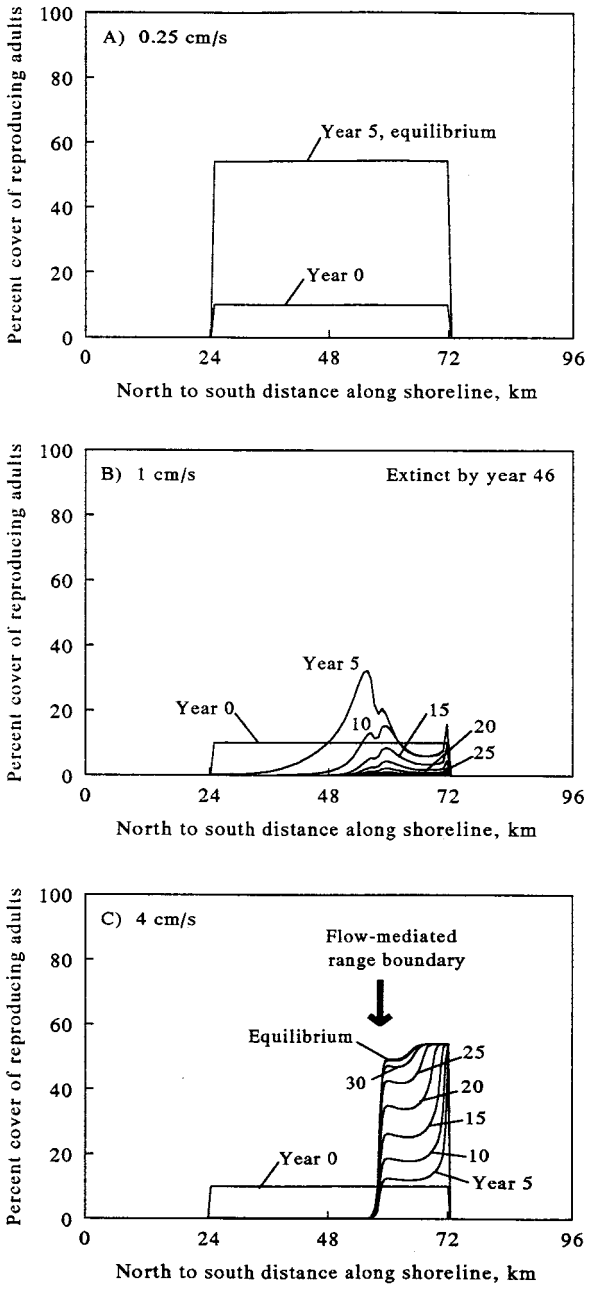

Figure 8: Adult shoreline distributions resulting from an eddy-circulation flow field. Note that populations can now persist when currents are rapid, but only in a subset of the suitable habitat; the bold arrow indicates this flow-induced range boundary.

Upstream Larval Input

Given the predicted existence of at least one oceanographic mechanism capable of yielding a persistent larval source (and given that there are likely others as well; see, e.g., Wolanski and Hamner 1988), this introduces the possibility that external input of larvae from upstream locations might alter the effects of different flow scenarios. This issue is explored for each of the four basic flow regimes in turn. In the case of the alongshore, converging, and eddy-circulation flow fields, a persistent source (which mimics the presence of a larval retention feature) is positioned next to the shoreline at the northern boundary. In the diverging flow situation (where a northern source would be expected to have little if any effect), larvae are assumed to originate from a site at the shore midway between the onshore jet and the northern edge of suitable habitat. The rate of larval input at a source is set to 1.1×10^{-5} m^{-2} s^{-1}, equivalent to a continuous net flux of 1 larva d^{-1} from each meter of coastline in the source region.

Alongshore Flow with a Source. Figure 9 demonstrates that an upstream larval source allows a population to resist more effectively the negative effects of alongshore advection. While the pattern of adult abundance in slow flows is identical to that found previously in the absence of external larval input, very different results arise at faster flows. At current speeds of 1 or 4 cm s^{-1}, adult populations persist throughout the suitable habitat range, although abundances vary markedly with distance from the source. Note that some of the flow-linked differences between figure 9*B* and 9*C* derive from the more effective entrainment of individuals from a larval source when velocities are faster.

Converging Flow with a Source. More intriguing patterns arise in the source-supplied converging flow situation (fig. 10*A*). For simplicity, we show only the 4 cm s^{-1} results for this and the two remaining flow fields. At this faster flow rate, while abundances still fall to 0 south of the jet, a northern source allows adults to persist in the northern half of suitable habitat. Thus, once again a purely flow-induced range boundary is established within the middle of uniformly suitable habitat.

Diverging Flow with a Source. Figure 10*B* shows the analogous results for the diverging flow field with 4 cm s^{-1} velocities. The addition of a larval source again prevents extinction and allows a population to persist along the coastline from the source to the downstream extent of suitable habitat. On the side of the onshore jet without a larval source, however, numbers of adults still decline through time to 0. Therefore this situation provides a third example of a purely flow-mediated range boundary.

Eddy Circulation with a Source. Unlike the other source-supplied flow scenarios, an eddy field with a northern source no longer induces range boundaries (fig. 10*C*), al-

though abundances continue to vary strikingly along the shore.

Discussion

The Potential for Flow-Induced Boundaries

Figures 8 and 10 suggest strongly that certain flow fields may be capable of generating range boundaries in benthic marine species with pelagic offspring, even in the absence of physiological, community, or habitat constraints (although such factors undoubtedly play interacting roles). Interestingly, such potential for flow-generated range structure may be unique to the sea. Terrestrial organisms that move long distances typically do so under their own power (often as adults), actively selecting where to go and in which habitats to live. Under these conditions, movement of the surrounding fluid is largely irrelevant for dispersal. Alternatively, in those cases where passive flow-induced dispersal takes place (e.g., as in wind-blown seeds or ballooning spiders), large differences in mass density between the transporting fluid (air) and the transported propagules greatly limits the duration those propagules can remain suspended above the ground and, therefore, also constrains the typical distances over which they can be carried (Denny 1993). This may ensure that most directional trends in passive terrestrial transport are obscured by short-term fluctuations in flow patterns (e.g., from weather or turbulence), preventing the establishment of robust fluid-mediated range boundaries.

Many marine systems may also operate in a somewhat curious manner from a metapopulations standpoint. In Levins's original (1969) framework, a broadly dispersing species would be expected to show high colonization rates to regions of empty but suitable habitat and exhibit relatively little sensitivity to the spatial arrangement of habitat. However, data presented above suggest that exactly the opposite situation may be typical of benthic marine organisms with dispersing larvae. Because of the directional nature of advective transport, the configuration of occupied habitat becomes critically important, interacting with the flow field to control relative rates of colonization and extinction among subpopulations along the shore.

Shapes of Distributions

Model results also suggest that coastal flows may affect adult abundance patterns within a range as well as setting range borders per se. Traditionally, abundance across a species' range is assumed to track local habitat quality (Brown 1984; Gaston 1990), with both quantities peaking at the center of the range. Consider, however, the equilibrium adult distribution of figure 10*A*, which shows an exponential decline toward the boundary. While this curve has precisely the shape one would expect based on an argument that fewer organisms subsist in poorer habitats near range edges, habitat quality in this study plays no role whatsoever in determining patterns of abundance.

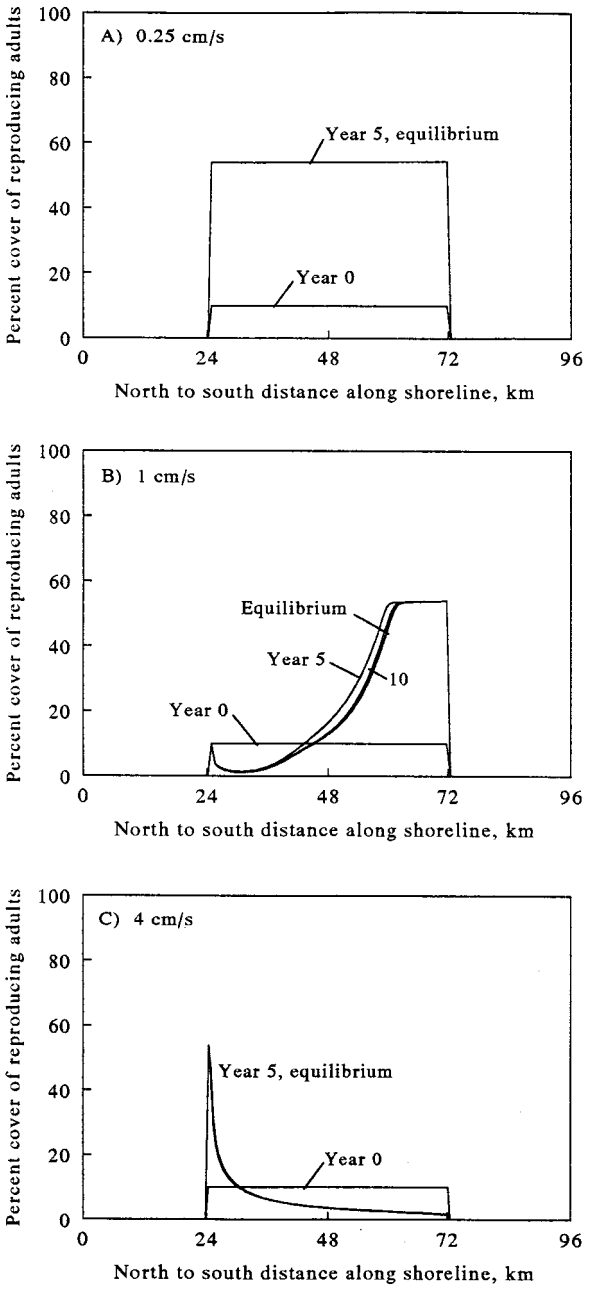

Figure 9: Adult shoreline distributions resulting from a uniform alongshore flow with a larval source positioned at the northern tip of shoreline. Note that populations are now able to persist even in the presence of rapid alongshore flows.

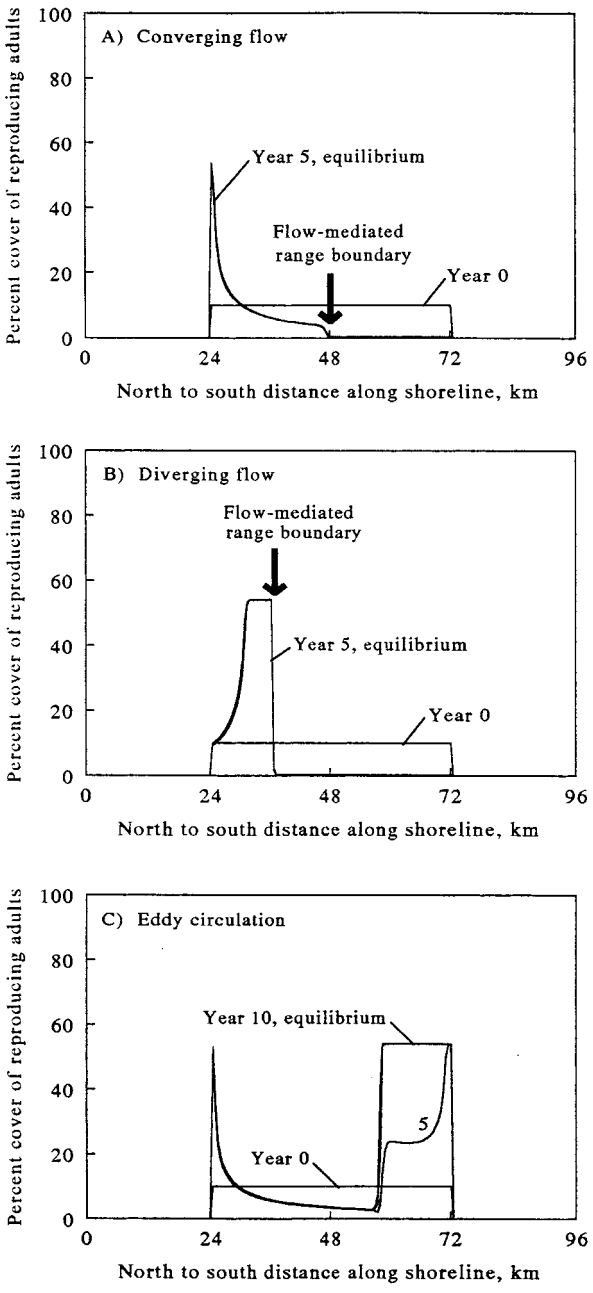

Figure 10: Adult shoreline distributions resulting from 4 cm s^{-1} converging, diverging, and eddy flow fields with larval sources. *A*, Distributions arising from a converging flow scenario with a source located at the northern tip of shoreline. *B*, Distributions arising from a diverging flow scenario with a source located midway between the northern tip of shoreline and the midpoint of suitable habitat. *C*, Distributions arising from a eddy-circulation flow scenario with a source again at the northern tip of habitat. Note the bold arrows indicating flow-induced range boundaries.

This point, coupled with the apparent wide variety of possible distributional patterns generated by currents (fig. 10), suggests that marine systems may deviate regularly from the rule that organism abundance tracks habitat quality.

Directionality of Boundaries

Perhaps one of the most important findings of this study is that flow-induced range boundaries can have directional bias (see fig. 11). With upstream larval input, converging and diverging flow fields function as two-way dispersal barriers. That is, larvae are transported in such a way that populations originally established north of the offshore/onshore jet are unable to invade regions south of the jet, and vice versa. Note that while data for the analogous southern-source cases are not shown explicitly, they work simply as mirror images of their complements.

In marked contrast, an eddy-circulation scenario leads to a unidirectional, one-way boundary (fig. 11*D*). A population in the north (or one that initially extends throughout the suitable habitat region) can expand into and persist in the southern half of habitat (fig. 8). If a northern larval source is supplied, the population will maintain itself across the entire shoreline where habitat exists (fig. 10*C*). However, a population originating south of the jet is unable to expand into the opposing current and is confined to regions below the offshore jet. This constraint is apparent from the fact that even when abundances are high in the south (as they are at equilibrium in fig. 8), no range extension occurs. Thus, although a species may be fully capable of living in the north physiologically, it is prevented from persisting there by oceanographic factors.

Point Conception along the central California coast of the United States is a major faunal break for many marine species and may, in fact, provide a real-world example of an eddy-circulation scenario. Along much of the coast north of Point Conception, throughout much of the year, the California Current flows southward, paralleling the shore (Hickey 1998). At Point Conception, the coastline turns suddenly from a north-south to an east-west orientation, and the California Current largely diverges from the shore as it continues southward. During spring and summer (the major reproductive season for most marine species in this region), northerly winds along the central California coast also produce coastal upwelling, and a strong and persistent upwelling jet or filament often extends south from Point Conception (Huyer 1983). Furthermore, as winds wrap around the point to enter the west end of the Santa Barbara Channel (fig. 12), a gradient in wind stress is established, with stronger westerly winds occurring offshore near the Channel Islands. In combination with buoyancy-driven flows entering the channel from the east, these factors drive a persistent recirculating

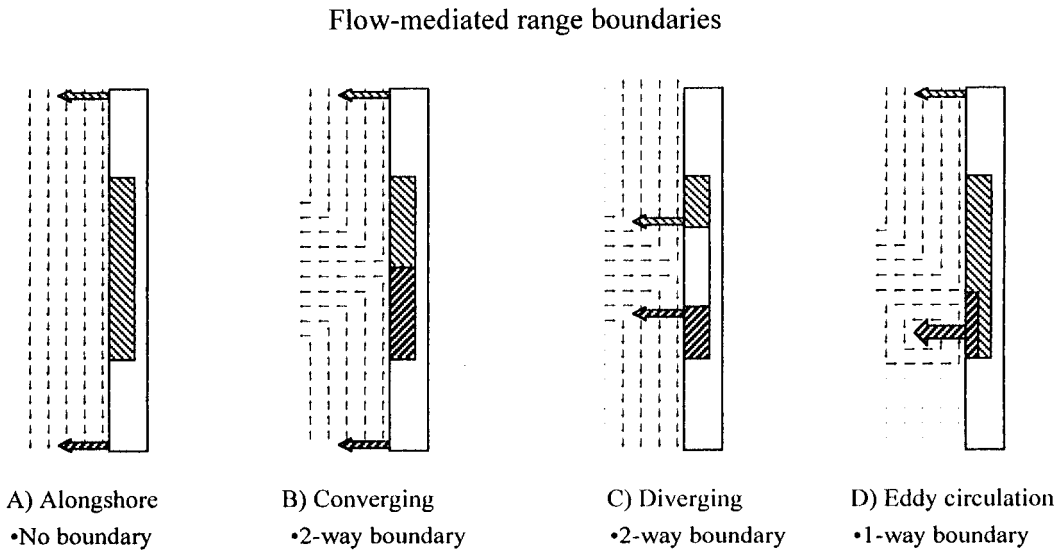

Figure 11: Schematic of potential flow-mediated range boundaries. *A*, No boundaries are produced in the middle of suitable habitat by simple uniform alongshore flow fields. *B*, Two-way range boundaries can be generated by converging flows with upstream larval sources since individuals produced in the north cannot invade regions in the south, and vice versa. *C*, Two-way range boundaries can also be generated by diverging flows with larval sources. *D*, One-way boundaries can be generated by eddy-circulation flow fields with larval sources. In this situation, individuals in the north can settle throughout the entire region of suitable habitat (allowing adults to persist everywhere), but larvae originating in the south cannot effectively cross the offshore jet to settle in the north, preventing a southern adult population from expanding northward.

eddy that sits in the west end of the channel throughout much of the time when marine species in the area are reproducing (Harms and Winant 1998). Figure 12 depicts this eddy.

Although the sudden shift in coastline orientation near Point Conception differs from the straight shore used in our theoretical representations, we nonetheless suggest that the eddy scenario of our model may approximate the spring/summer flow field described above. The analogy is perhaps most easily seen by mentally rotating the east-west portion of the coastline in figure 12 clockwise about Point Conception until it aligns vertically with the northern section of the shore. Although at this stage we hesitate to make too much of this comparison, there are some data that hint that this crude equivalency may be valid. Valentine (1966), Horn and Allen (1978), Murray and Littler (1981), and S. D. Gaines (unpublished data) suggest that Point Conception indeed functions as a one-way boundary, in the direction predicted by our model. That is, Point Conception allows relatively consistent north-south range continuity but commonly prevents expansion of southern species around it to the north. Note that such directional bias is more difficult to explain using standard temperature-based arguments (see, e.g., Valentine 1966) but arises naturally from a consideration of the links between flow and ocean dispersal.

Temporal Variability in Flow

While we find these correlations between model predictions and field observations tantalizing, we also emphasize that many central California species with dispersing larvae do not show northern range limits at Point Conception (while others show southern limits there; Morris et al. 1980). However, this is not surprising. There are numerous spatially varying factors associated with interacting currents that have the potential to modulate species' susceptibility to flow-induced boundaries. Such factors include not only physiological constraints but shifts in densities of important community players, substrate type, wave exposure, or changes in growth rates from differences in nutrient levels or suspended food concentrations, for example.

It is also possible that temporal variability in a flow field itself may alleviate its tendency to create a stringent range boundary. Because local extinctions typically take several years, and because a massive recruitment event can occur in a single season, one flow breakdown every few years

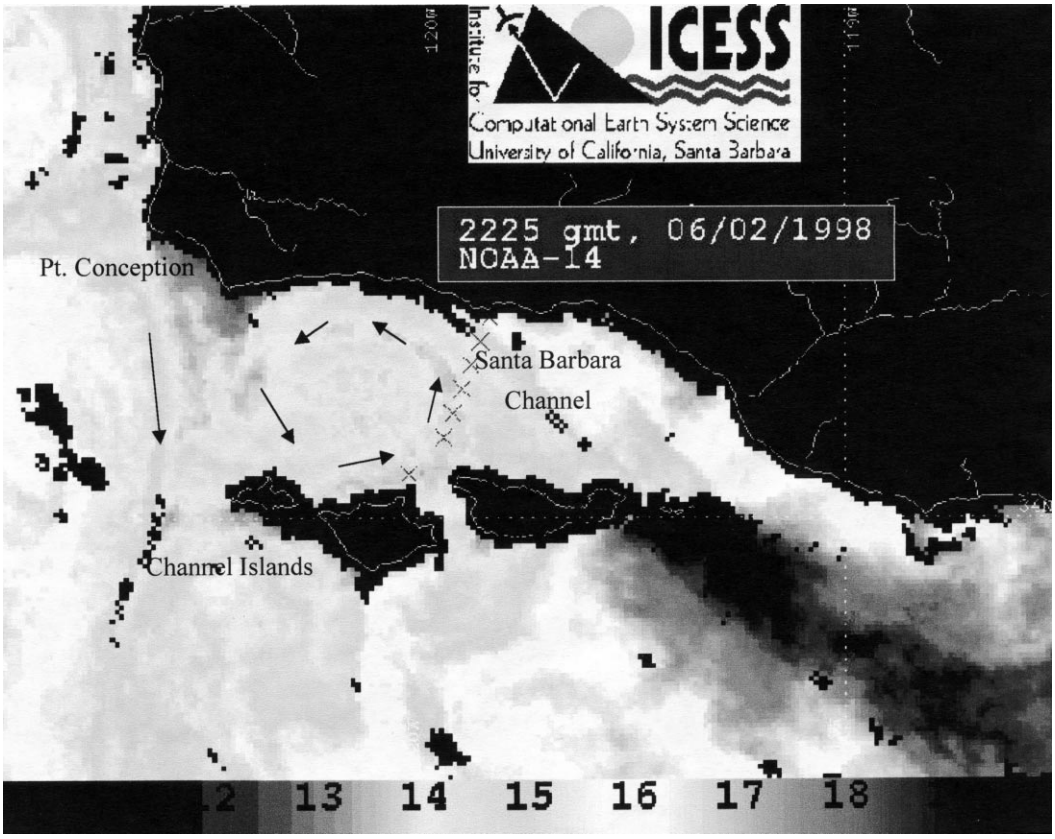

Figure 12: Satellite sea surface temperature image showing the recirculating eddy that persists through much of the spring and summer in the lee of Point Conception on the central California coast. In analogy to the diagram of figure 11*D*, this coastal region functions as a one-way biogeographic boundary.

may be sufficient to allow a population to persist where it otherwise could not if the flow were constant. In this way, flow variability can change an impenetrable barrier into one that is leaky. Depending on the degree of leakiness, a species may or may not become limited in range at any particular flow discontinuity. Figure 13 shows a simple example of how flow variability and persistence may be linked. Data in this figure are generated by reversing a 1 cm s^{-1} alongshore flow every 6 or 12 yr. The reversed flow field is assumed to last one reproductive season (during which its speed is held at 0.25 cm s^{-1}) before returning to normal. Under these simplified conditions, populations persist if flow reversals occur frequently enough. Although abundances decline between each reversal, the periodicity can reach a steady state. Note that it may be possible for such population cycling to occur in association with anomalous flows generated by El Niño–Southern Oscillation (ENSO) events (effects of which can be detected, for example, along the west coast of North America; Rienecker and Mooers 1986). In such a case, climatic factors might encourage range expansions not only because of temperature-linked effects but also via the ability of flow reversals to offset abundance declines in remnant populations by encouraging more frequent recruitment.

Life-History Implications

It is also clear that particular life-history features can interact with current regimes to make organisms more or less susceptible to dispersal barriers. For example, figure 14*A* shows the effects, in a simple alongshore flow field, of changing the precompetency and competency durations. If larval durations are increased from 3 wk to 5 wk, populations become much more vulnerable to extinction. In contrast, if the capacity for dispersal is reduced such that $d_1 = d_2 = 1$ wk, adults persist on the shore up to considerably faster flow rates.

Similarly, adult mortality rates also interact with current speed (fig. 14*B*). As adult death rates decline, populations

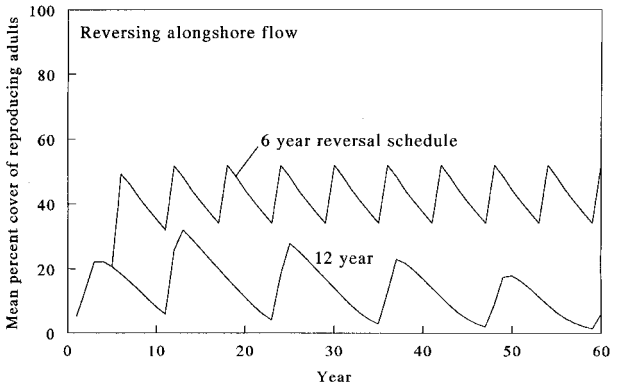

Figure 13: Influence of flow reversal on the persistence of a benthic population with dispersing larvae subjected to alongshore currents of 1 cm s^{-1}. With a reversal every 6 yr, a population can persist indefinitely at steady state, although abundances decline between each reversal event. If the reversal frequency is decreased to once every 12 yr, however, the population shows a long-term decrease (superimposed on shorter-term variation) that leads to eventual extinction.

can persist in the face of increasingly faster velocities. We see, however, that shifts in larval duration alter more strongly a species' sensitivity to alongshore flow than shifts in adult mortality rate. Note also the relatively sharp threshold for extinction; populations on this shoulder show nonuniform distributions with highest abundances at downstream locations.

Together the data of figure 14 indicate that predictions regarding range limits must be made with some knowledge of the reproductive biology and demographics of a given species. In general, results suggest that species with longer larval durations and/or higher adult mortality rates may be more susceptible to flow-induced boundaries than species with low dispersal potential and higher survivorship. Note, however, that timescales associated with specific flow fields (e.g., periods of revolution around eddy components of different sizes) have the potential to interact with life-history traits to produce quite complicated flow-dispersal relationships. Additional coupling may also exist between currents, their associated temperature gradients, and dispersal caused by the dependence of rates of larval development on temperature.

Retention Features and Coastal Processes

The above model results are based on organism biology, flow fields, coastline topography, and physics of transport that have been vastly simplified. While this simplicity is deliberate and (in our view) a strength of the approach, it also indicates that caution should be employed when interpreting results. In particular, we note that our model predicts population extinctions occurring at improbably slow flows, apparent from the fact that marine organisms live ubiquitously on coasts where velocities routinely exceed speeds used in our simulations. Note, however, that although this mismatch may initially appear unsettling, it is to be expected for at least two reasons and does not affect the major conclusions of this study.

Model oversensitivity to flow is expected first from the way we have ignored effects of shoreline irregularity. In reality, coastal topography often retards alongshore transport by generating retention features of a spectrum of sizes, durations, and efficiencies. Heuristically, we picture a scenario where larvae become successively entrained in channels, embayments, and eddy fields, progressing in a rather saltatory way down a coastline (see also Denny and Humphrey 1989; Denny et al. 1992). If included in our model, such retention mechanisms would ameliorate (to a certain

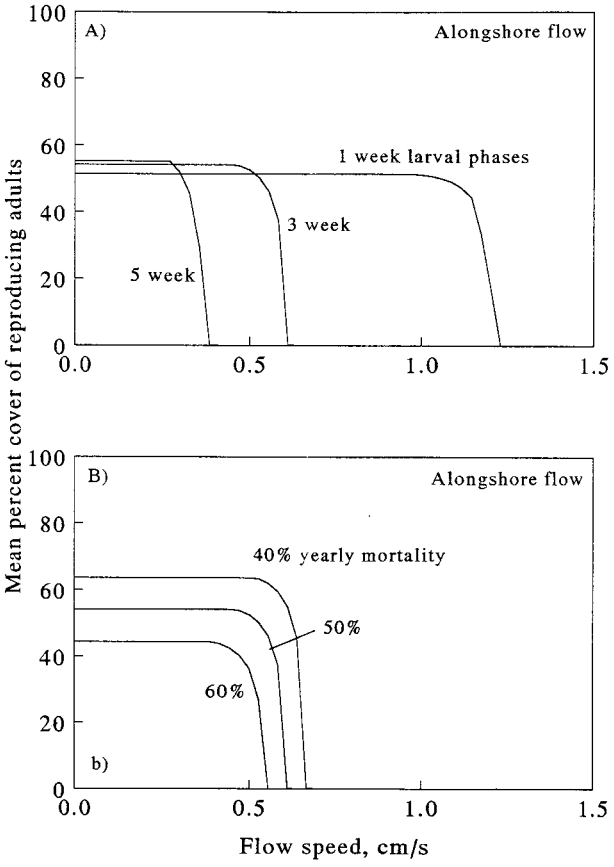

Figure 14: Influence of life-history traits on the persistence of a benthic population with dispersing larvae subjected to alongshore currents. *A*, As the duration of larval precompetency and competency periods lengthens, the population can persist only in the face of relatively slower currents. *B*, As adult mortality rates climb, the population can persist only in the face of relatively slower currents.

extent) consequences of alongshore flow by increasing rates at which larvae settle back into their original source populations.

Second, we reemphasize that our model parameterizes turbulent diffusion in a simplified way. For example, we have used a constant eddy diffusivity, whereas a more proper (but more complicated) representation would have K increasing offshore (e.g., Webb 1999). Furthermore, we have neglected consequences of shear dispersion (Bowden 1965) in a coastal boundary layer that can cause alongshore "stretching" of a larval cloud (note that PRG do incorporate components of this effect). Since it is dispersive processes that allow larvae to spread in opposition to a current, and because our idealized flow fields and diffusivity tend to reduce the efficacy of diffusion, an increased sensitivity to advection results. Note, however, that this increased sensitivity is a second-order effect; even if K is much larger, currents retain their ability to determine distributional pattern. This point is verified by dimensional analysis and an exploration of parameter space that indicate that the Peclet number, $\mathrm{Pe} = vl/K$, an index of the relative importance of advective and diffusive transport, dominates model dynamics (l is a length scale estimated as vd_1, the mean transport distance during a larva's precompetency period). When Pe is held constant and the diffusivity increased, critical flow speeds rise, and spatial gradients in abundance flatten, but overall trends remain the same. In other words, a smaller K essentially just decreases the threshold speeds at which currents begin to affect distributional pattern. Because a constant Pe dictates that $v \propto K^{1/2}$, critical flow speeds associated with larger (but realistic) K's still fall well within the range of those observed in nature.

We also note that this model has avoided consideration of more complex cross-shore phenomena that may carry larvae shoreward and, therefore, partially ameliorate consequences of alongshore advection and dilution. The upwelling and relaxation processes examined by Alexander and Roughgarden (1996) provide an obvious example. Work by Shanks (1983), Pineda (1991), and Leichter et al. (1996) have also implicated surface slicks from internal waves and breaking internal bores in cross-shore movement of larvae. Shanks (1995) provides a review of additional mechanisms. Larval behavior may, in addition, enable individuals to exploit vertical gradients in flow magnitude and direction (e.g., Hill 1991*b*) or, among strongly swimming species, to track a variety of environmental cues (e.g., Wolanski et al. 1997). This could potentially influence both cross-shore and alongshore transport. More fundamentally, actual flow fields are complex and three dimensional, and there is also temporally varying patchiness associated with turbulence that does not appear in advective-diffusion solutions describing time-averaged means. We note here that our lack of inclusion of such processes should not be construed as a form of disregard for their potential importance. Rather, what we have intended to accomplish in this study is to explore in a general context the ability of major current features to impose range boundaries in marine species. As noted earlier, these predictions will most assuredly be modified by other physical, physiological, behavioral, and ecological factors.

Conclusions

Despite the presence of a multitude of interacting factors influencing species distribution, results outlined here suggest that nearshore oceanographic features can affect strongly patterns of range in benthic marine species with dispersing larvae. It is also probably not entirely coincidental that several of the simple flow fields predicted by this study to generate range limits are associated with biogeographic boundaries in nature. Such flow-induced dispersal barriers appear to have the potential to act (depending on the current regime) as one- or two-way limits to range and may be more effective for some species than others (depending on interactions between life-history characteristics and current variability). This apparent capacity of flow to generate constraints on range may reflect a largely overlooked distinction between biological systems on land and in the sea.

Acknowledgments

We thank M. W. Denny, H. Possingham, R. Sagarin, and two anonymous reviewers for valuable discussions and feedback and the Institute for Computational Earth System Science at the University of California at Santa Barbara for satellite imagery. This is contribution 15 of the Partnership for Interdisciplinary Studies of Coastal Oceans: A Long-Term Ecological Consortium funded by the David and Lucile Packard Foundation. Additional support was provided by the Andrew W. Mellon Foundation, the Department of Energy National Institute for Global Environmental Change, the Keck Foundation, the National Center for Ecological Analysis and Synthesis working group on species borders, and National Science Foundation grant OCE 9813983 to S.D.G.

APPENDIX A

Estimation of *c*, the Settlement Coefficient

Gaines et al. (1985) recorded settlement rates of the order 1×10^4 individuals m^{-2} wk^{-1} when larval concentrations in the water at the shore were 50 individuals m^{-3} and 1×10^3 individuals m^{-2} wk^{-1} when concentrations were about 25 individuals m^{-3}. Assuming that larvae were carried predominantly at the surface in the top 1 m of water (i.e., equating per area concentrations with per volume estimates), and given that $A = 1$ m^2 m^{-1} (meaning that the larval flux to a square meter of substrate is identical to the flux across each meter of coastline), we compute settlement coefficients ranging between approximately 3×10^{-4} s^{-1} and 5×10^{-5} s^{-1} (i.e., c equals the measured settlement rate divided by A and the recorded value of L).

APPENDIX B

Computational Method

Equations (1)–(3) are solved numerically using finite difference techniques. An alternating direction implicit (ADI) splitting method (Ferziger 1981) is applied to equation (1), and a trapezoidal implicit routine is used for equation (2). Overall, the coupled equations are solved over a spatial mesh of grid points incrementally through time. Details are sketched below.

The first and second spatial derivatives of equation (1) are approximated at each grid point using a central difference scheme:

$$\begin{aligned}
\frac{\partial L_{i,j}}{\partial x} &\cong \frac{L_{i+1,j} - L_{i-1,j}}{2\Delta x}, \\
\frac{\partial L_{i,j}}{\partial y} &\cong \frac{L_{i,j+1} - L_{i,j-1}}{2\Delta y}, \\
\frac{\partial^2 L_{i,j}}{\partial x^2} &\cong \frac{L_{i+1,j} - 2L_{i,j} + L_{i-1,j}}{(\Delta x)^2}, \\
\frac{\partial^2 L_{i,j}}{\partial y^2} &\cong \frac{L_{i,j+1} - 2L_{i,j} + L_{i,j-1}}{(\Delta y)^2},
\end{aligned} \tag{B1}$$

where i and j are the grid indices in the x and y directions, (running from 1 to M and 1 to N), respectively. Oceanic borders of the solution space correspond to $i = 1$, $j = 1$, and $j = N$, while the shoreline corresponds to $i = M$.

The temporal derivative is approximated by

$$\frac{L_{i,j}^{n+1} - L_{i,j}^{n}}{\Delta t} \cong \frac{1}{2}\left(K\frac{\partial^2 L_{i,j}^{n}}{\partial x^2} - u_{i,j}\frac{\partial L_{i,j}^{n}}{\partial x} - \lambda L_{i,j}^{n} + K\frac{\partial^2 L_{i,j}^{n+1}}{\partial x^2} - u_{i,j}\frac{\partial L_{i,j}^{n+1}}{\partial x} - \lambda L_{i,j}^{n+1}\right) + K\frac{\partial^2 L_{i,j}^{n+1/2}}{\partial y^2} - v_{i,j}\frac{\partial L_{i,j}^{n+1/2}}{\partial y}, \tag{B2}$$

where integer superscripts represent sequential time steps ($n = 1, 2, 3, \ldots$). This approximation corresponds to a combined application of a trapezoid rule (in x) and a midpoint rule (in y). Defining

$$a_x = \frac{K}{2(\Delta x)^2},$$

$$a_y = \frac{K}{2(\Delta y)^2},$$

$$b_x(i,j) = \frac{u_{i,j}}{4\Delta x}, \tag{B3}$$

$$b_y(i,j) = \frac{v_{i,j}}{4\Delta y},$$

and with some rearrangement and substitution from equation (B1), (B2) can be split into two separate steps, a *y*-sweep and an *x*-sweep. The *y*-sweep is

$$([-a_y - b_y]\Delta t)L_{i,j-1}^{n+1/2} + (1 + 2a_y\Delta t)L_{i,j}^{n+1/2} + ([-a_y + b_y]\Delta t)L_{i,j+1}^{n+1/2} =$$

$$([a_x + b_x]\Delta t)L_{i-1,j}^{n} + \left(1 - 2a_x\Delta t - \frac{\lambda}{2}\Delta t\right)L_{i,j}^{n} + ([a_x - b_x]\Delta t)L_{i+1,j}^{n}; \tag{B4}$$

The *x*-sweep is

$$([-a_x - b_x]\Delta t)L_{i,j-1}^{n+1} + \left(1 + 2a_x\Delta t + \frac{\lambda}{2}\Delta t\right)L_{i,j}^{n+1} + ([-a_x + b_x]\Delta t)L_{i,j+1}^{n+1} =$$

$$([a_y + b_y]\Delta t)L_{i-1,j}^{n+1/2} + (1 - 2a_y\Delta t)L_{i,j}^{n+1/2} + ([a_y - b_y]\Delta t)L_{i+1,j}^{n+1/2}. \tag{B5}$$

Although the sum of equations (B4) and (B5) is equivalent to (B2), each sweep has a tridiagonal form that can be solved efficiently using standard matrix algorithms. First, $L_{i,j}$ is computed over all j for each i, yielding estimates for $L(x, y)$ at an intermediate time step, then $L_{i,j}$ is computed over all i for each j, producing $L(x, y)$ a full time step later.

Temporal changes in adult density are represented by

$$\frac{B_j^{n+1} - B_j^n}{\Delta t} = \frac{1}{2}\left(\frac{\partial B_j^n}{\partial t} + \frac{\partial B_j^{n+1}}{\partial t}\right). \tag{B6}$$

Substituting from equation (2), using central differencing analogous to equation (B1), and rearranging yields

$$\left(1 + [caL_{M,j}^{n+1} + \mu]\frac{\Delta t}{2}\right)B_j^{n+1} = \left(1 - [caL_{M,j}^{n} + \mu]\frac{\Delta t}{2}\right)B_j^{n} + \frac{cA\Delta t}{2}\left(L_{M,j}^{n+1} + L_{M,j}^{n}\right), \tag{B7}$$

which can be solved as a matrix for B_j over all j at time $n + 1$.

Equations (B4), (B5), and (B7) are coupled through the boundary condition of equation (3). When central differenced and rearranged, equation (3) yields

$$L_{M+1,j} = \frac{2\Delta x m}{K}B_j - \frac{2\Delta x c F_j}{K}L_{M,j} + L_{M-1,j}, \tag{B8}$$

where $L_{M+1,j}$ is a fictitious point landward of the shoreline. The right-hand side of equation (B8) replaces $L_{M+1,j}$ (which appears because of the central differencing) in the shoreline boundary elements of the matrices of equations (B4) and (B5). Absorbing boundaries at the oceanic borders of the solution space correspond to $L_{0,j} = L_{i,0} = L_{i,N+1} = 0$; thus, all other boundary elements remain unmodified.

Because there are products of B and L in equations (B7) and (B8) (via F), equations (B4), (B5), and (B7) cannot

be solved directly simultaneously. Therefore, an iterative routine is used. Values of $L_{M,j}$ and B_j at time step n provide good starting guesses for values at $n + 1$; thus, a simple replacement strategy achieves convergence typically within one or two iterations.

At grid locations where flow trajectories show right-angle turns, the standard finite differencing in the advective terms no longer represents gradients along streamlines and must be modified. There are four such cases:

For a N→W or E→S corner, respectively, central difference approximations to the advective terms become:

$$u_{i,j}\frac{\partial L_{i,j}}{\partial x} \cong u_{i,j}\frac{L_{i,j-1} - L_{i-1,j}}{(\Delta x + \Delta y)},$$

$$v_{i,j}\frac{\partial L_{i,j}}{\partial y} \cong v_{i,j}\frac{L_{i-1,j} - L_{i,j-1}}{(\Delta x + \Delta y)}.$$

Similarly, for a N→E or W→S turn, respectively,

$$u_{i,j}\frac{\partial L_{i,j}}{\partial x} \cong u_{i,j}\frac{L_{i+1,j} - L_{i,j-1}}{(\Delta x + \Delta y)},$$

$$v_{i,j}\frac{\partial L_{i,j}}{\partial y} \cong v_{i,j}\frac{L_{i+1,j} - L_{i,j-1}}{(\Delta x + \Delta y)}.$$

For a S→W or E→N turn, respectively,

$$u_{i,j}\frac{\partial L_{i,j}}{\partial x} \cong u_{i,j}\frac{L_{i,j+1} - L_{i-1,j}}{(\Delta x + \Delta y)},$$

$$v_{i,j}\frac{\partial L_{i,j}}{\partial y} \cong v_{i,j}\frac{L_{i,j+1} - L_{i-1,j}}{(\Delta x + \Delta y)}.$$

Finally, for a S→E or W→N corner, respectively,

$$u_{i,j}\frac{\partial L_{i,j}}{\partial x} \cong u_{i,j}\frac{L_{i+1,j} - L_{i,j+1}}{(\Delta x + \Delta y)},$$

$$v_{i,j}\frac{\partial L_{i,j}}{\partial y} \cong v_{i,j}\frac{L_{i,j+1} - L_{i+1,j}}{(\Delta x + \Delta y)}.$$

These modifications alter slightly coefficients in the matrices of equations (B4) and (B5) but do not disturb their tridiagonal character. Note that in the converging, diverging, and eddy-circulation flow fields, nonzero magnitudes of u and v are always set equal to insure that fluid mass is conserved.

Literature Cited

Alexander, S. E., and J. Roughgarden. 1996. Larval transport and population dynamics of intertidal barnacles: a coupled benthic/oceanic model. Ecological Monographs 66:259–275.

Bowden, K. F. 1965. Horizontal mixing in the sea due to a shearing current. Journal of Fluid Mechanics 21: 83–95.

Briggs, J. C. 1974. Marine biogeography. McGraw-Hill, New York.

Brown, J. H. 1984. On the relationship between abundance and distribution of species. American Naturalist 124: 255–279.

Caley, M. J., M. H. Carr, M. A. Hixon, T. P. Hughes, G. P. Jones, and B. A. Menge. 1996. Recruitment and the local dynamics of open marine populations. Annual Review of Ecology and Systematics 27:477–500.

Clarke, A. 1993. Temperature and extinction in the sea: a physiologist's view. Paleobiology 19:499–518.

Connell, J. H. 1961. The influence of interspecific competition and other factors on the distribution of the barnacle *Chthamalus stellatus*. Ecology 42:710–723.

Connolly, S. R., and J. Roughgarden. 1998. A latitudinal

gradient in northeast Pacific intertidal community structure: evidence for an oceanographically based synthesis of marine community theory. American Naturalist 151:311–326.

Denny, M. W. 1993. Air and water: the biology and physics of life's media. Princeton University Press, Princeton, N.J.

Denny, M. W., and J. Humphrey. 1989. Fluid mechanical constraints on biotic functions. Mechanical Engineering 111:50–53.

Denny, M. W., J. Dairiki, and S. Distefano. 1992. Biological consequences of topography on wave-swept rocky shores. I. Enhancement of external fertilization. Biological Bulletin (Woods Hole) 183:220–232.

Etter, R. J., and H. Caswell. 1994. The advantages of dispersal in a patchy environment: effects of disturbance in a cellular automaton model. Pages 284–305 *in* C. M. Young, ed. Reproduction, larval biology, and recruitment of the deep-sea benthos. Columbia University Press, New York.

Ferziger, J. H. 1981. Numerical methods for engineering application. Wiley, New York.

Gaines, S. D., and M. D. Bertness. 1992. Dispersal of juveniles and variable recruitment in sessile marine species. Nature (London) 360:579–580.

Gaines, S. D., and J. Lubchenco. 1982. A unified approach to marine plant-herbivore interactions. II. Biogeography. Annual Review of Ecology and Systematics 13: 111–138.

Gaines, S., S. Brown, and J. Roughgarden. 1985. Spatial variation in larval concentrations as a cause of spatial variation in settlement for the barnacle, *Balanus glandula*. Oecologia (Berlin) 67:267–272.

Gaston, K. J. 1990. Patterns in the geographical ranges of species. Biological Reviews 65:105–129.

Harms, S., and C. D. Winant. 1998. Characteristic patterns of circulation in the Santa Barbara Channel. Journal of Geophysical Research 103:3041–3065.

Hayden, B. P., and R. Dolan. 1976. Coastal marine fauna and marine climates of the Americas. Journal of Biogeography 3:71–81.

Hedgpeth, J. W. 1957. Marine biogeography. Pages 359–382 *in* J. W. Hedgpeth, ed. Treatise on marine ecology and paleoecology. Geological Society of America Memoirs 67. Geological Society of America, Boulder, Colo.

Hickey, B. M. 1998. Coastal oceanography of western North America from the tip of Baja California to Vancouver Island. Sea 11:345–393.

Hill, A. E. 1991*a*. Advection-diffusion-mortality solutions for investigating pelagic larval dispersal. Marine Ecology Progress Series 70:117–128.

———. 1991*b*. A mechanism for horizontal zooplankton transport by vertical migration in tidal currents. Marine Biology 111:485–492.

Hines, A. H. 1978. Reproduction in three species of intertidal barnacles from central California. Biological Bulletin (Woods Hole) 154:262–281.

Horn, M. H., and L. G. Allen. 1978. A distributional analysis of California coastal marine fishes. Journal of Biogeography 23–42.

Hutchins, L. W. 1947. The bases for temperature zonation in geographical distribution. Ecological Monographs 17: 325–335.

Huyer, A. 1983. Coastal upwelling in the California current system. Progress in Oceanography 12:259–284.

Jablonski, D., and R. A. Lutz. 1983. Larval ecology of marine benthic invertebrates: paleobiological implications. Biological Reviews of the Cambridge Philosophical Society 58:21–89.

Jackson, G. A., and R. R. Strathmann. 1981. Larval mortality from offshore mixing as a link between precompetent and competent periods of development. American Naturalist 118:16–26.

Leichter, J. J., S. R. Wing, S. L. Miller, and M. W. Denny. 1996. Pulsed delivery of subthermocline water to Conch Reef (Florida Keys) by internal tidal bores. Limnology and Oceanography 41:1490–1501.

Levins, R. 1969. Some demographic and genetic consequences of environmental heterogeneity for biological control. Bulletin of the Entomological Society of America 15:237–240.

Loder, J. W., B. Petrie, and G. Gawarkiewicz. 1998. The coastal ocean of northeastern North America: a large-scale view. Sea 11:105–133.

Longhurst, A. 1995. Seasonal cycles of pelagic production and consumption. Progress in Oceanography 36: 77–167.

Mann, K. H., and J. R. N. Lazier. 1996. Dynamics of marine ecosystems. 2d ed. Blackwell Science, Cambridge, Mass.

McGowan, J. A. 1971. Oceanic biogeography of the Pacific. Pages 3–74 *in* B. M. Funnell and W. R. Riedel, eds. The micropalaeontology of oceans. Cambridge University Press, Cambridge.

Menge, B. A., B. A. Daley, P. A. Wheeler, E. Dahlhoff, E. Sanford, and P. T. Strub. 1997. Benthic-pelagic links and rocky intertidal communities: bottom-up effects on top-down control? Proceedings of the National Academy of Sciences of the USA 94:14530–14535.

Morris, R. H., D. P. Abbott, and E. C. Haderlie. 1980. Intertidal invertebrates of California. Stanford University Press, Stanford, Calif.

Murray, S. N., and M. M. Littler. 1981. Biogeographical analysis of intertidal macrophyte floras of southern California. Journal of Biogeography 8:339–351.

Okubo, A. 1971. Oceanic diffusion diagrams. Deep-Sea Research 18:789–802.

Palmer, A. R., and R. R. Strathmann. 1981. Scale of dispersal in varying environments and its implications for life histories of marine invertebrates. Oecologia (Berlin) 48:308–318.

Pianka, E. R. 1988. Evolutionary ecology. 4th ed. Harper & Row, New York.

Pickard, G. L., and W. J. Emery. 1990. Descriptive physical oceanography. 5th ed. Butterworth Heinemann, Oxford.

Pielou, E. C. 1979. Biogeography. Wiley, New York.

Pineda, J. 1991. Predictable upwelling and the shoreward transport of planktonic larvae by internal tidal bores. Science (Washington, D.C.) 253:548–551.

Pond, S., and G. L. Pickard. 1983. Introductory dynamical oceanography. Pergamon, New York.

Possingham, H. P., and J. Roughgarden. 1990. Spatial population dynamics of a marine organism with a complex life cycle. Ecology 71:973–985.

Pyefinch, K. A. 1948. Notes on the biology of Cirripedes. Journal of the Marine Biological Association of the United Kingdom 27:465–503.

Rapoport, E. H. 1982. Areography: geographical strategies of species. Pergamon, New York.

Rienecker, M. M., and C. N. K. Mooers. 1986. The 1982–1983 El Nino signal off Northern California. Journal of Geophysical Reasearch 91:6597–6608.

Richards, S. A., H. P. Possingham, B. J. Noye. 1995. Larval dispersion along a straight coast with tidal currents: complex distribution patterns from a simple model. Marine Ecology Progress Series 122:59–71.

Rohde, K., M. Heap, and D. Heap. 1993. Rapoport's rule does not apply to marine teleosts and cannot explain latitudinal gradients in species richness. American Naturalist 142:1–16.

Roughgarden, J., and Y. Iwasa. 1986. Dynamics of a metapopulation with space-limited subpopulations. Theoretical Population Biology 29:235–261.

Roughgarden, J., S. Gaines, and H. Possingham. 1988. Recruitment dynamics in complex life cycles. Science (Washington, D.C.) 241:1460–1466.

Roy, K., D. Jablonski, and J. W. Valentine. 1994. Eastern Pacific molluscan provinces and latitudinal diversity gradient: no evidence for "Rapoport's rule." Proceedings of the National Academy of Sciences of the USA 91: 8871–8874.

———. 1998. Marine latitudinal diversity gradients: tests of causal hypotheses. Proceedings of the National Academy of Sciences of the USA 95:3699–3702.

Scheltema, R. S. 1971. The dispersal of the larvae of shoal-water benthic invertebrate species over long distances by ocean currents. Pages 7–28 *in* D. J. Crisp, ed. Fourth European marine biology symposium. Cambridge University Press, Cambridge.

Shanks, A. L. 1983. Surface slicks associated with tidally forced internal waves may transport pelagic larvae of benthic invertebrates and fishes shoreward. Marine Ecology Progress Series 13:311–315.

———. 1995. Mechanisms of cross-shelf dispersal of larval invertebrates and fish. Pages 323–367 *in* L. R. McEdward, ed. Ecology of marine invertebrates. CRC, Boca Raton, Fla.

Stevens, G. C. 1989. The latitudinal gradient in geographical range: how so many species coexist in the Tropics. American Naturalist 133:240–256.

———. 1996. Extending Rapoport's rule to Pacific marine fishes. Journal of Biogeography 23:149–154.

Strathmann, M. F. 1987. Reproduction and development of marine invertebrates of the northern Pacific coast. University of Washington Press, Seattle.

Strub, P. T., J. M. Mesias, V. Montecino, J. Rutllant, and S. Salina. 1998. Coastal ocean circulation off western South America. Sea 11:273–313.

Suchanek, T. H., J. B. Geller, B. R. Kreiser, and J. B. Mitton. 1997. Zoogeographic distributions of the sibling species *Mytilus galloprovincialis* and *M. trossulus* (Bivalvia: Mytilidae) and their hybrids in the north Pacific. Biological Bulletin (Woods Hole) 193:187–194.

Thorson, G. 1950. Reproductive and larval ecology of marine bottom invertebrates. Biological Reviews of the Cambridge Philosophical Society 25:1–45.

Valentine, J. W. 1966. Numerical analysis of marine molluscan ranges on the extratropical northeastern Pacific shelf. Limnology and Oceanography 11:198–211.

Van den Hoek, C. 1975. Phytogeographic provinces along the coasts of the northern Atlantic Ocean. Phycologia 14:317–330.

Webb, D. J. 1999. An analytic model of the Agulhas Current as a western boundary current with linearly varying viscosity. Journal of Physical Oceanography 29: 1517–1527.

Wolanski, E., and W. M. Hamner. 1988. Topographically controlled fronts in the ocean and their biological influence. Science (Washington, D.C.) 241:177–181.

Wolanski, E., P. Doherty, and J. Carleton. 1997. Directional swimming of fish larvae determines connectivity of fish populations on the Great Barrier Reef. Naturwissenschaften 84:262–268.

Wroblewski, J. S., and J. J. O'Brien. 1981. On modeling the turbulent transport of passive biological variables in aquatic ecosystems. Ecological Modeling 12:29–44.

Associate Editor: Hugh Possingham